Article

Not peer-reviewed version

A Computational Fluid Dynamics-Based Design Optimization Tool for Carbon Capture Enclosure

Md Shariful Alam * and Narjes Abbasabadi

Posted Date: 27 March 2026

doi: 10.20944/preprints202603.2179.v1

Keywords: direct air capture; computational fluid dynamics; carbon positive solutions; climate responsive architecture; sustainable design; nature-based solutions; design computation

Article

A Computational Fluid Dynamics-Based Design Optimization Tool for Carbon Capture Enclosure

Md Shariful Alam * and Narjes Abbasabadi

Department of Architecture, College of Built Environments, University of Washington; nabbasab@uw.edu
* Correspondence: malam60@gatech.edu

Abstract

Decarbonizing the built environment is crucial for achieving global sustainability goals, as buildings and infrastructure contribute significantly to carbon emissions. This study explores integrating direct air carbon capture, utilizing CaCO3-based technologies, into urban buildings through passive sustainable design. A computational framework was developed to optimize architectural design and enclosure geometry for enhanced passive airflow, using mass flow rate as a proxy for carbon absorption potential. Implemented within Rhino3D and Grasshopper using Ladybug and Eddy3D, the workflow integrates weather data and CFD simulation to compute segmented mass flow rates through stacked capture trays. The framework simplifies traditionally complex CFD processes by introducing a custom segmented mass-flow calculation approach that enables comparative performance assessment during early-stage design. Results confirm the validity of the proposed workflow, revealing that façade rotation can modify total mass flow by up to 96.5%, seasonal wind variability can cause airflow to range from approximately 8.5 kg/s in January to 169.5 kg/s in May in Seattle, and tower shadowing can reduce flow by up to 60.9%, demonstrating the strong influence of enclosure design and spatial configuration on passive carbon capture potential. This research establishes a performance-driven design framework that enables architectural geometry to actively enhance passive carbon capture integration, positioning building design as a measurable contributor to climate mitigation strategies.

Keywords: direct air capture; computational fluid dynamics; carbon positive solutions; climate responsive architecture; sustainable design; nature-based solutions; design computation

---

1. Introduction

As global temperatures continue to rise, reducing atmospheric CO_2 concentrations has become an urgent scientific and policy priority. While sustainable design strategies mitigate operational and embodied emissions, emerging carbon removal technologies offer an essential complementary pathway. Direct Air Capture (DAC) is a highly scalable approach that extracts CO_2 directly from ambient air; however, conventional active DAC systems rely on mechanical fans and costly synthetic sorbents [1–4]. To overcome these financial and energetic barriers, recent innovations have shifted toward passive, mineral-based DAC systems. These systems utilize an abundantly available calcium-based cyclic carbonation process: calcium carbonate ($CaCO_3$) is thermally decomposed into calcium oxide (CaO), hydrated to calcium hydroxide ($Ca(OH)_2$), and then exposed to ambient air. Driven by prevailing wind currents rather than mechanical fans, the $Ca(OH)_2$ reacts with atmospheric CO_2 to reform $CaCO_3$ through a passive mineralization process. Because this approach relies entirely on natural ventilation, the carbonation reaction rate depends critically on airflow exposure and mass transfer dynamics. Consequently, the aerodynamic distribution of air within DAC enclosures emerges as a vital determinant of overall system efficiency [5–7].

 doi:10.20944/preprints202603.2179.v1

Despite the importance of natural ventilation in passive DAC, limited research has explored how architectural enclosure design can be optimized to enhance airflow. While the internal chemistry of mineral-based capture technologies is highly engineered, comparatively little attention has been given to the enclosure's geometric capacity to improve air exposure without increasing mechanical energy demand. Beyond merely providing structural protection from the elements, the enclosure actively regulates wind distribution across the stacked capture assemblies. Identifying aerodynamic configurations that maximize air exchange—and thereby optimize CO_2 contact with the sorbent materials—remains a critical blind spot, particularly as these systems scale toward site-specific architectural integrations. To address this, a rigorous computational framework is necessary to evaluate enclosure performance under varying climatic conditions using quantitative metrics. This study builds upon existing Computational fluid dynamics (CFD)-based architectural workflows and proposes a computational framework tailored to carbon capture enclosure design, employing mass flow rate as a primary objective function while acknowledging the limitations inherent in simplified simulation approaches.

CFD tools are essential for simulating and visualizing airflow behavior within architectural enclosures. Over the past decades, various CFD applications have been integrated with computer-aided design (CAD) platforms to support performance-informed design workflows[8–12]. Examples include Autodesk Flow Design (now retired), which functioned as a virtual wind tunnel for visual airflow analysis, and Autodesk CFD, which provides more advanced simulation capabilities [13]. Other platforms such as Rhino CFD and Microflow extend airflow simulation to Rhino and SketchUp environments, respectively, while cloud-based platforms like SimScale offer web-based CFD analysis [14]. However, many of these tools are not fully optimized for parametric design environments that enable iterative exploration of large geometric design spaces. For this reason, a CFD integration compatible with Grasshopper-based parametric modeling was prioritized in this study to support systematic performance-driven design exploration.

Applying CFD to architectural models presents specific challenges, particularly in mesh generation. Architectural geometries are often complex and non-watertight, complicating their conversion into the closed volumetric domains required for accurate CFD analysis [15]. To address such issues, hybrid meshing strategies that combine structured and unstructured elements have been proposed to balance computational efficiency and simulation accuracy, especially during early-stage design exploration. CFD tools integrated within parametric design environments, such as Butterfly and Eddy3D—both based on the OpenFOAM solver—offer automated meshing workflows [16,17]. While both platforms facilitate airflow simulation within design interfaces, differences in computational architecture influence performance; Butterfly relies primarily on CPU-based processing, whereas Eddy3D incorporates GPU acceleration, enabling faster solution times. Given the iterative nature of the design exploration undertaken in this study, computational efficiency was a critical consideration, and the accelerated simulation capability of Eddy3D supported rapid evaluation of multiple geometric configurations.

The reliability of Eddy3D has been supported through empirical validation studies. Simulated wind velocity and mean radiant temperature outputs have been compared with field measurements from multiple on-campus monitoring stations, demonstrating strong agreement between predicted and observed environmental conditions [18,19]. Additionally, Eddy3D-derived wind fields have been incorporated into a Universal Thermal Climate Index (UTCI) framework, where correlations were identified between simulated thermal comfort conditions and observed cycling activity [20].

Recent research has expanded the integration of Eddy3D within data-driven and optimization-based design workflows. Automated Eddy3D pipelines have been used to generate CFD training datasets for surrogate modeling, enabling near-instantaneous airflow predictions during early-stage massing exploration with reported SSIM values between 75–97% across 564 urban geometries [21]. Similarly, Eddy3D outputs have been embedded in parametric and machine-learning–assisted multi-objective optimization frameworks combining artificial neural networks and genetic algorithms [22]. Model-based optimization approaches have also been implemented using tools such as Opossum to

 doi:10.20944/preprints202603.2179.v1

explore high-rise building form generation without surrogate modeling [23]. At the neighborhood scale, Grasshopper-based optimization frameworks combining Ladybug tools and Eddy3D have been used to explore trade-offs between building energy performance and outdoor thermal comfort autonomy [11]. Parallel tool-development research has extended toward coupled urban microclimate simulations; for example, urbanMicroclimateFoam has been validated against real-world data with temperature RMSE around ~1 °C and relative humidity errors below 5%, highlighting ongoing efforts to integrate coupled microclimate physics into the evolving Eddy3D ecosystem [10].

Although Eddy3D is built upon the OpenFOAM simulation engine, certain fluid dynamic parameters—such as mass flow rate—are not directly accessible through its interface, as the tool primarily focuses on visualizing airflow patterns related to building massing and orientation. Consequently, no established workflow currently enables the quantitative evaluation of passive airflow performance for building-integrated DAC systems within commonly used parametric design environments. This limitation restricts the integration of aerodynamic performance considerations during early-stage architectural design.

DAC systems that rely on natural airflow require controlled wind distribution through stacked calcium hydroxide capture assemblies, making mass flow rate a critical parameter for evaluating carbon absorption potential. Since airflow distribution is influenced by enclosure geometry, tray configuration, and wind conditions, variations in architectural design can significantly affect system performance. To address this methodological gap, this study develops a computational framework implemented in Rhino3D and Grasshopper that integrates site-specific climatic analysis (Ladybug) with steady-state airflow simulation (Eddy3D).

The study contributes to the field in two ways: (1) it formalizes a CFD-integrated parametric workflow tailored to building-integrated DAC systems by introducing a segmented mass-flow evaluation approach that bridges architectural geometry and airflow performance metrics; and (2) it demonstrates the applicability of this method through scenario-based investigations, illustrating how enclosure geometry influences airflow redistribution in passive DAC configurations. These contributions position enclosure design as a quantifiable variable within performance-driven carbon capture integration strategies. The framework enables designers to evaluate enclosure performance using quantifiable airflow metrics, supporting performance-informed integration of carbon capture systems in architectural design.

2. Methodology

This paper aims to illustrate the process of calculating mass flow rate under specific site conditions, using a representative location near downtown Seattle, WA, USA. In this study, airflow and mass flow rate are used as proxy indicators for potential carbon capture performance, since increased airflow across the calcium hydroxide trays increases the contact between air and sorbent material, thereby improving the potential for CO_2 absorption. To focus on the impact of the architectural geometry itself, the simulations were intentionally simplified by assuming a flat terrain with no surrounding obstacles or adjacent buildings—effectively excluding complex external environmental parameters. This assumption enabled a clear, unobstructed evaluation of how the proposed enclosure influences airflow and supports passive carbon capture performance. NOAA wind data, typically preferred for wind planning due to its higher accuracy and multi-year datasets, was not available for Seattle. In its absence, TMYx data was utilized for this study as it provides a comprehensive record of typical meteorological conditions for the location. While TMYx data is not typically weighted for wind direction analysis, it was rationalized for this specific context to represent wind conditions in downtown Seattle. To minimize the limitations of TMYx data, only the most prevailing wind direction was prioritized for simulations. The least frequent wind direction and seasonal variations, though included in preliminary analysis, were not emphasized in simulation-based optimization, as they hold limited relevance for practical design purposes. This ensures that any recommended building design, informed by Eddy3D projections, is optimized for typical conditions. In our case, the prevailing wind predominantly originates from the northwest throughout

Preprints.org (www.preprints.org) | NOT PEER-REVIEWED | Posted: 27 March 2026 doi:10.20944/preprints202603.2179.v1

most of the year. This directional data, represented as a vector, along with the associated speed, extracted as a float, are utilized to conduct CFD analysis using Eddy3D. This approach enables more accurate simulations of site-specific wind flow. Additionally, if the building is surrounded by objects that may impact the microclimate, they should be accounted for during simulations in Eddy3D.

A linear building orientation, aligned in a north-south direction, is envisioned for the site, with stacked trays of calcium hydroxide ($Ca(OH)_2$) positioned within (see Figure 1). The design prioritizes larger facades on the east and west sides, with the south side designated for entry and the north side considered opaque. These prescribed conditions amplify the uncertainties regarding wind direction within the structure, thereby yielding a range of mass flow rate values. The building dimensions are set at 40m by 20m with a height of 12m, devoid of surrounding objects exceeding a height of 0.01m. Initially, only one stack of tray, standing at a height of 10m, is considered for preliminary studies. However, owing to the unknown distribution and configuration of stacked trays, a segmented analysis of the entire tower is conducted (see Figure 2). It's important to note that the rectangular distribution of towers yields varying mass flow rates around them, as demonstrated in the results section, attributed to wind diversion by bordering towers.

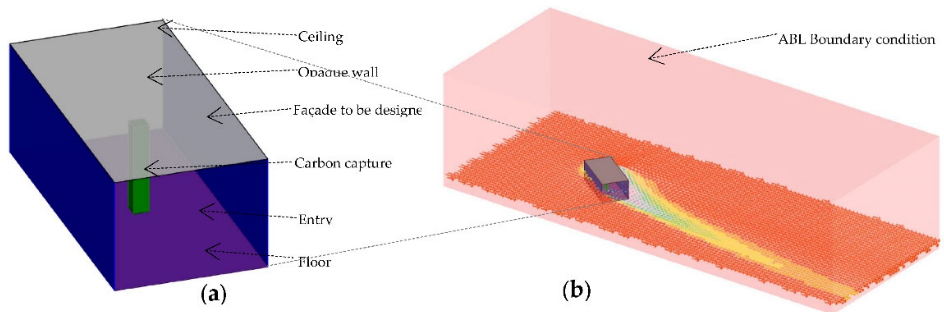

Figure 1. (**a**)Considered structure for the research; (**b**) simulated airflow for the most prevailing wind direction.

While exploring multiple design iterations the team followed constant simulation configuration to generate more accurate configuration (see Table 1). The virtual boundary condition is a box shaped ABL (atmospheric boundary layer). The box's height is set to default from Eddy3D. On both sides of the shorter length, the design is maintained at twice its breadth. We have twice as much length in the windward direction and four times as much length in the leeward direction in the larger length [24]. Given that the structure analyzed (40m x 20m x 12m) is significantly smaller than the domain height, the default setting ensured sufficient room for airflow modeling without interference from artificial boundary effects. This approach is consistent with best practices for CFD simulations, where the domain height typically exceeds the model dimensions to allow accurate simulation of wind profiles and turbulence effects.

While customizing the domain height might have allowed for further refinement, it was deemed unnecessary in this case, as the focus was on analyzing airflow behavior within and around the structure, rather than simulating far-field wind effects. Future studies may consider domain customization to investigate specific site conditions requiring a tighter computational domain. Simulation properties are fixed from the precedent study for CFD simulations done by Eddy3D [20]. Only the height of the surface roughness has been changed to 0.01m considering the site is nearly level and has few obstructions facing the windward direction. The number of iterations is set at 1000 since most simulations revealed that this range allowed for convergence. For a detailed examination, we took into account a substantial number of probing points.

Table 1. Simulation and Building Input Parameters Used in Eddy3D Analysis.

Category	Parameter	Value	Notes
Building	Building footprint	40 m × 20 m	Rectangular plan
Geometry	Building height	12 m	Height of the enclosure structure

	Stack height	10 m	DAC trays stack within the structure.
	Tray dimensions	2 m × 2 m	Assumed per tray
	Tray distribution	Uniform segmentation	10 segments (see Figure 2)
	Orientation	North-South	Long facades face East-West
Simulation Setup	Wind direction	Northwest	Prevailing direction (from TMYx analysis)
	Wind speed	Derived from TMYx	Annual average at 10m height
	Reference height	10 m	Common for urban wind profile input
	Surface roughness height	0.01 m	Flat, unobstructed terrain assumption
	Boundary condition	ABL (Atmospheric Boundary Layer)	Cylindrical domain in Eddy3D
	Turbulence model	k-Epsilon	Eddy3D default
	Number of iterations	1000	Ensured convergence across cases
	Probing points per block segment	16	Cross-section sampling points per tray segment
Meshing Control	Acc feature	3	Mesh refinement for feature edges; validated in precedent
	Acc ground	3	Ground-level refinement; improves boundary-layer accuracy
Solver Settings	Relaxation factor	Optimized	Damping factor for stable convergence (default by Eddy3D)
	Solution and algorithm control	Optimized	Auto-schemes for solver control in OpenFOAM backend
Environmental Data	Climate dataset	TMYx (Seattle, WA)	Used in Ladybug for weather analysis
	Surroundings	None	Flat site with no contextual buildings
	Terrain type	Flat	No elevation changes

From Eddy3D, we gain insights solely into wind velocity at specific probing points. It's imperative to assess airflow adequacy at individual stacks of trays. Averaging the velocities across all probing points fails to elucidate the volume of wind passing through. Additionally, wind direction is expected to alter upon encountering obstacles. The number of stacks stacked atop one another in a column is contingent upon equipment engineering. We considered each tray to be square, with a length of 2m. Given the dynamic physics of the designed structure, uniform airflow throughout the entire block is unrealistic. To deepen our comprehension, we've subdivided the block into 10 parts and are evaluating the mass flow rate for each segment (see Figure 2).

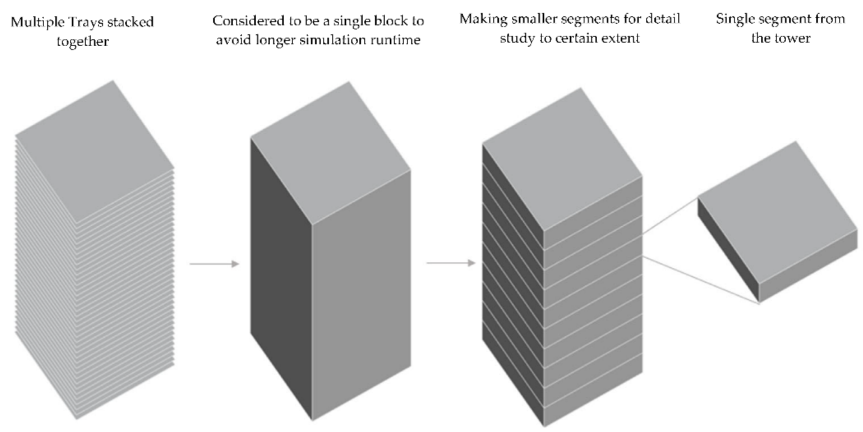

Figure 2. Segmented analysis of the tower of stacked trays.

While running the simulation, the cross-sectional area of all the blocks was reduced to half to account for the air resistance caused by the stack of trays. These geometries simulate both the diversion and resistance effects introduced by the stack. Modeling individual trays in detail within the CFD setup, while feasible, would significantly increase computational demand due to the larger number of CFD cells required. To mitigate this computational expense, the team recommends simplifying the simulation by reducing the effective wind speed passing through the trays, which inherently reflects the reduction in carbon absorption caused by resistance. This approach balances computational efficiency with the need to provide actionable insights for design optimization.

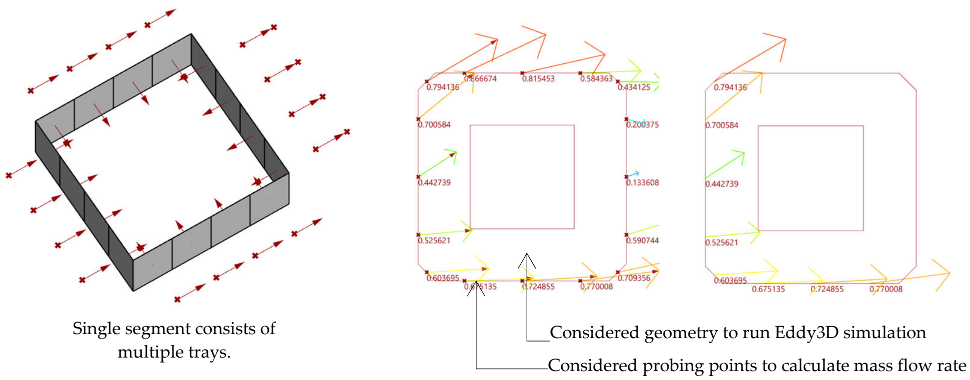

Figure 3. (a) Wind vectors and surface vectors, (b) negating wind vectors that have a 0 or negative cosine.

To calculate the mass flow rate after simulation, actual-sized blocks are considered. While it's an open system, it's hard to calculate accurately the flow of air through each block portion. Assuming that each block portion is a sink and wind coming from all possible directions. Each side of the block portion is divided into four divisions. These divisions are considered the cross sections through which wind is going inside or coming out. We have taken the centroids of these cross sections as our probing points. So, each block has 16 probing points, and each block has 160 probing points.

Now if we run Eddy3D simulation, we can get the wind direction and speed at those points. With extracted values, we can calculate the mass flow rate at each point. Each cross-section is considered as a vector surface having an inward direction. While calculating the mass flow rate, the angle between the surface direction and the wind vector extracted from Eddy3D at its centroid is considered. If the angle is zero degrees, it indicates the wind is passing through the block. If the angle is 90 degrees or more, it means that the wind is either coming out of the block or not entering it. Any probing point having a negative cosine is avoided (see Figure 3). Because the sum of all the mass flow rates at all considered cross sections will be zero for both winds going inside and coming out. Only the mass flow rate of the cross sections having wind passing through is considered. Thinking that the viscosity of the air is negligible, we have not considered it in our equation.

$$m = \rho . v . A . cos\,\theta \tag{1}$$

$$m = \left(\frac{P}{RT}\right) * M * v * A * cos\,\theta \tag{2}$$

$$Total\ flow = \sum \left(\frac{P_n}{R_n . T_n}\right) * M . v_n . A_n . cos\,\theta_n \tag{3}$$

where:

v = flow speed (m/s)
A = cross-sectional area (m2)
ϱ = mass density of the fluid (1.293 kg/m3 for air)
m = mass flow rate (kg/s)
P = pressure of the gas
T = temperature of the gas
M = molecular weight of the gas
R = universal gas constant

Preprints.org (www.preprints.org) | NOT PEER-REVIEWED | Posted: 27 March 2026 doi:10.20944/preprints202603.2179.v1

Equation 1-3. Formulas used to calculate mass flow rate, starting from the basic density-based equation (1), incorporating ideal gas assumptions (2), and extended to a segmented multi-vector summation for total flow (3).

The density of air is influenced by atmospheric pressure (P) and temperature (T). For this study, we assumed the air density to be constant for any period of time. However, the team recommends extracting monthly average atmospheric pressure and temperature from the TMYx file using Ladybug for more accurate simulations (see Figure 4). When the most prevailing wind direction is considered, the average wind pressure and temperature of the site for the whole year can be utilized for the calculation. In the equation for calculating mass flow rate, the molecular weight of air and the universal gas constant are both constants. Ladybug provided the values for P and T, while the cross-sectional area (A) was obtained from our model. The wind speed (v) and direction (cosθ) were determined using Eddy3D. It is worth noting that reducing the cross-sectional area allows for a more accurate calculation of the mass flow rate, but it also results in increased computation time.

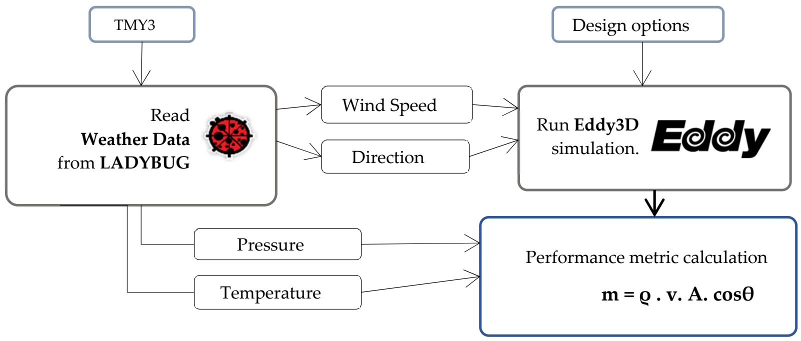

Figure 4. Framework developed for this study.

By integrating the relevant variables into our calculations (see Equation 1-3), we computed the mass flow rate across defined probing points. Subsequently, we visualized the total mass flow rate across individual segments of the tower using colour coding, providing a clear spatial representation of airflow variation. To test whether the workflow produces meaningful, physically consistent results, we simulated three distinct scenarios. In Scenario 1, we rotated operable façade panels, hypothesizing that alignment with wind direction would increase mass flow rate. Scenario 2 examined seasonal wind speed variations, where higher wind months were expected to produce greater airflow. Scenario 3 introduced multiple towers, with the expectation that mass flow would decrease in towers positioned further from the windward edge due to shielding. These scenarios allow us to assess whether the workflow responds predictably to known aerodynamic principles, thereby validating its usefulness in early-stage carbon capture enclosure design. Figure 5 provides an overview of the full methodological workflow described in this section.

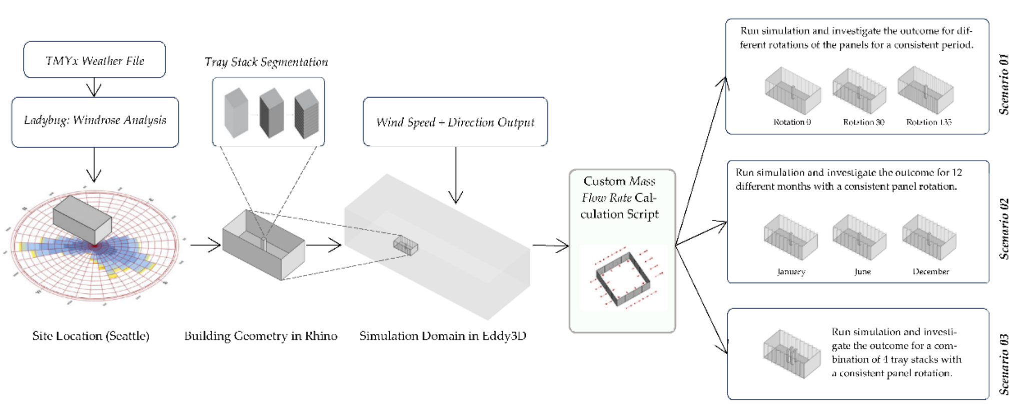

Figure 5. Workflow diagram showing the step-by-step methodological process used in this study.

Preprints.org (www.preprints.org) | NOT PEER-REVIEWED | Posted: 27 March 2026 doi:10.20944/preprints202603.2179.v1

3. Results

The following results illustrate how the proposed workflow captures variations in airflow and mass flow rate across three distinct design scenarios. Each simulation explores how changes in geometry or environmental conditions influence performance within the established system:

3.1. Scenario 1: Operable Façade Option

For this scenario, operable vertical fins were placed on the longer sides of the façade facing east and west. These panels can be rotated from 0 to 180 degrees to adjust the aperture (see Figure 6). The assumption is that aligning the panel orientation with the wind direction will maximize wind harnessing, thereby increasing CO_2 absorption (considered average wind speed of 6.0575 m/s from the north-west direction). Figure 7 shows wind flow visualization around the tower at a height of 6.5 meters above the ground. Figure 9 illustrates the mass flow rate for individupal segments of the tower with varying orientations of the vertical fins. The visualizations clearly indicate that greater apertures lead to increased wind flow around the tower (see Figure 8).

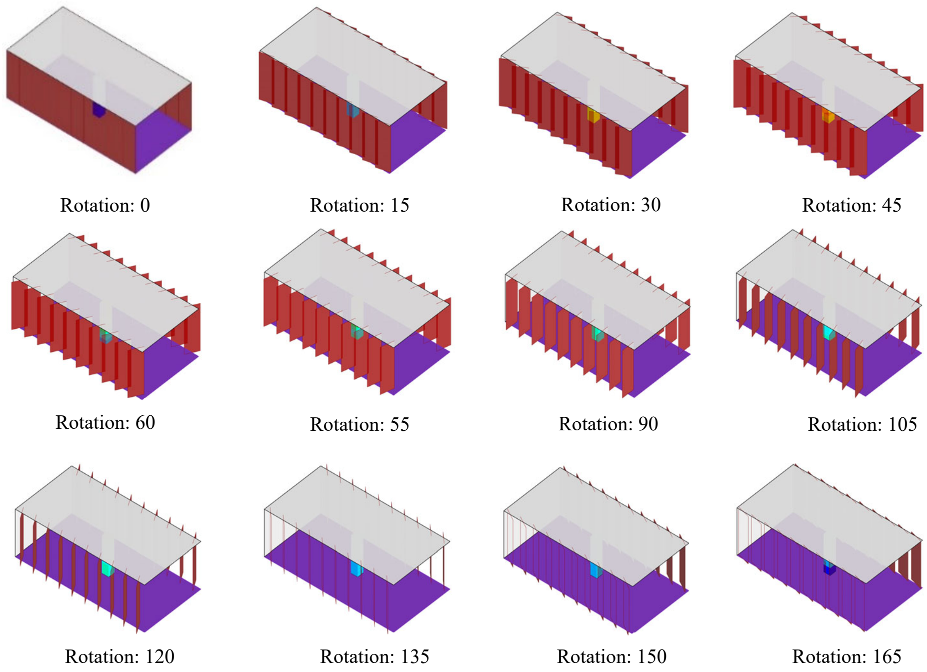

Figure 6. Considered structure at different rotations of vertical panels.

 doi:10.20944/preprints202603.2179.v1

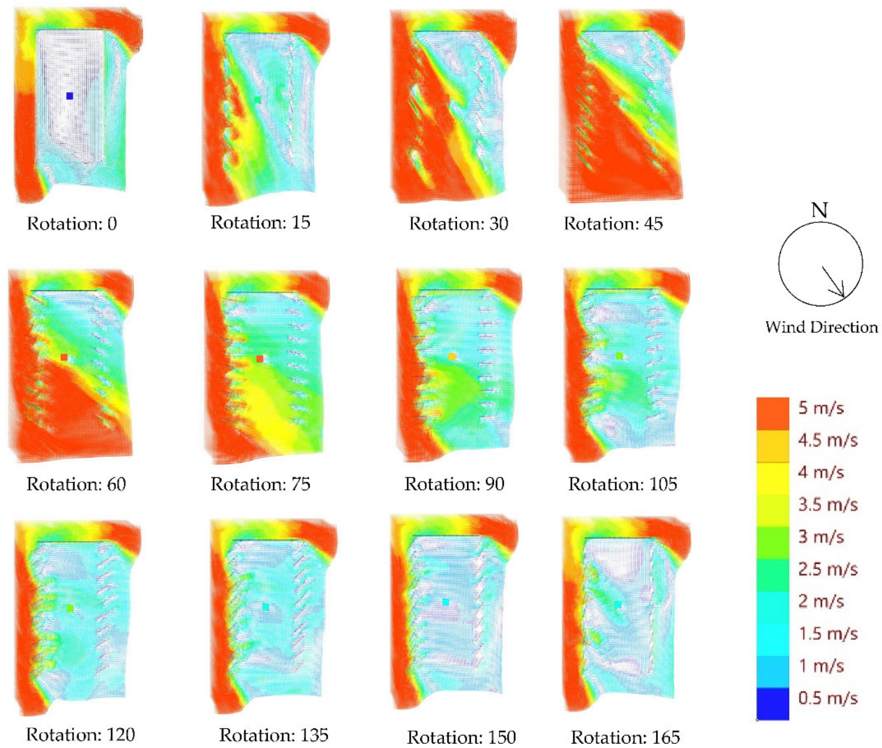

Figure 7. Wind flow analysis at different rotations of vertical panels.

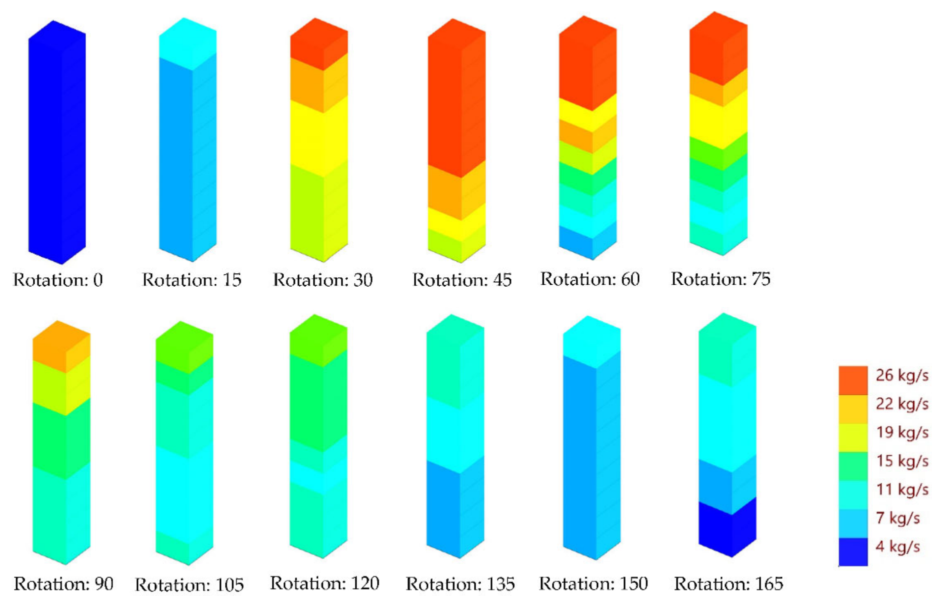

Figure 8. Heatmap of mass flow rate for different segments of the tower.

Preprints.org (www.preprints.org) | NOT PEER-REVIEWED | Posted: 27 March 2026 doi:10.20944/preprints202603.2179.v1

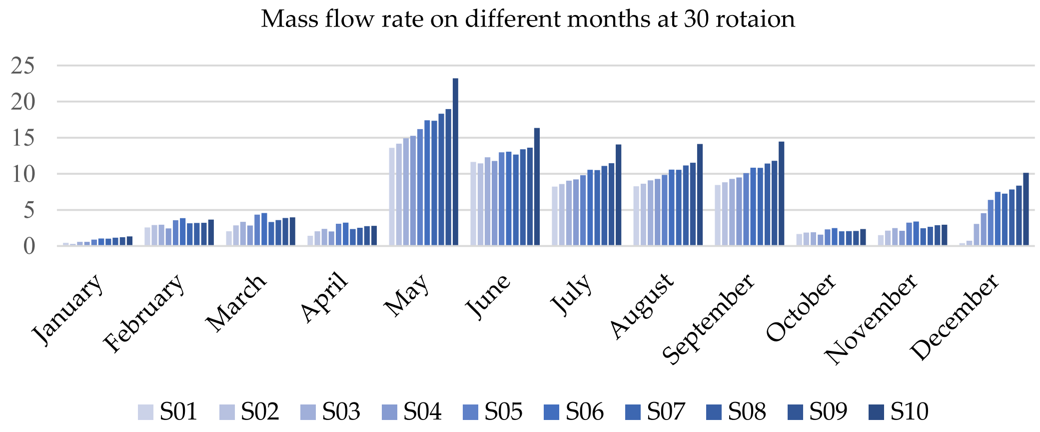

Figure 9. Mass flow rates at different rotations for the tower.

3.2. Scenario 02: Constant Panel Rotation Across Months

From the previous investigation, it was observed that a moderate amount of wind could be harnessed when the orientation of the vertical fins was set to negative 30 degrees relative to the north-south direction. While this wind direction is prevalent for most of the year, it is crucial to investigate how performance varies across different months when wind direction and speed change. The assumption is that the mass flow rate around the towers will fluctuate throughout the year.

Figure 10 visualizes wind flow for different months, reflecting the most prevalent wind direction during those times. Figure 11 illustrates the changes in mass flow rate around the tower due to varying wind speeds and directions. Figure 12 provides a more detailed understanding of the tower's performance across different conditions, offering insights to improve and refine design solutions.

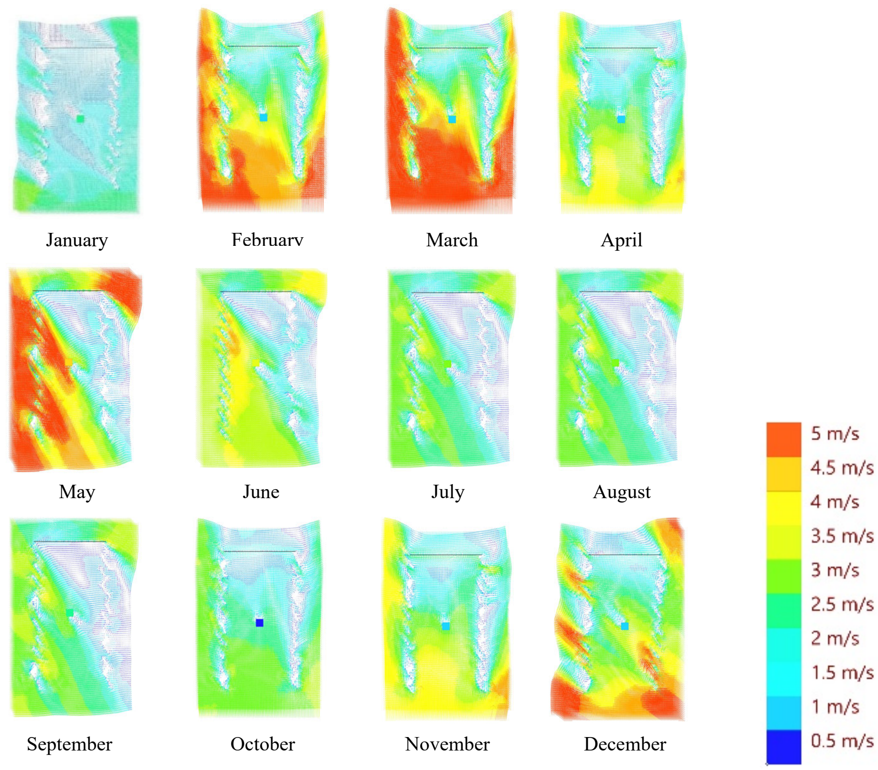

Figure 10. Wind flow analysis for different months of the year.

 doi:10.20944/preprints202603.2179.v1

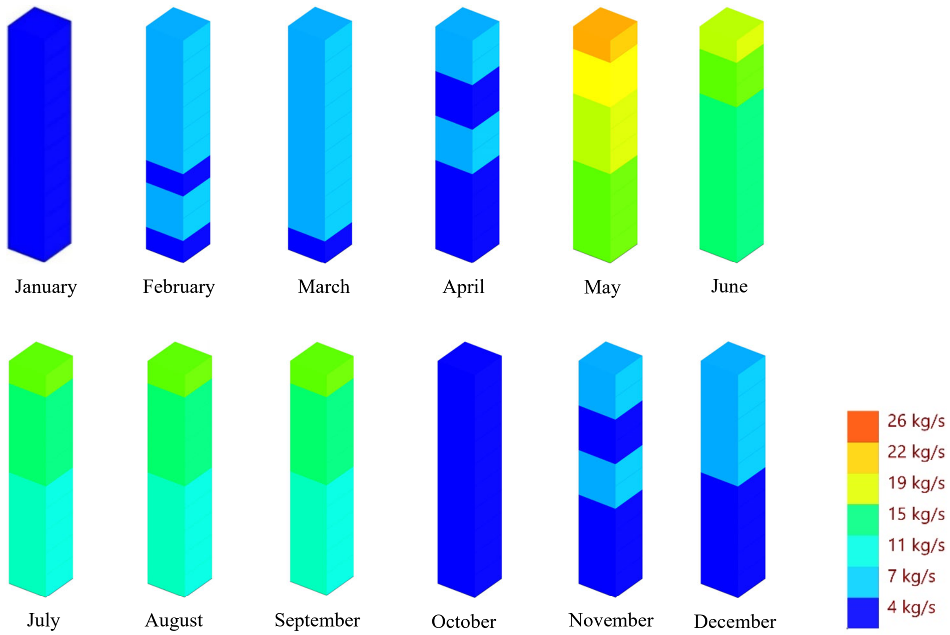

Figure 11. Heatmap of mass flow rates of different segments of the tower on different months.

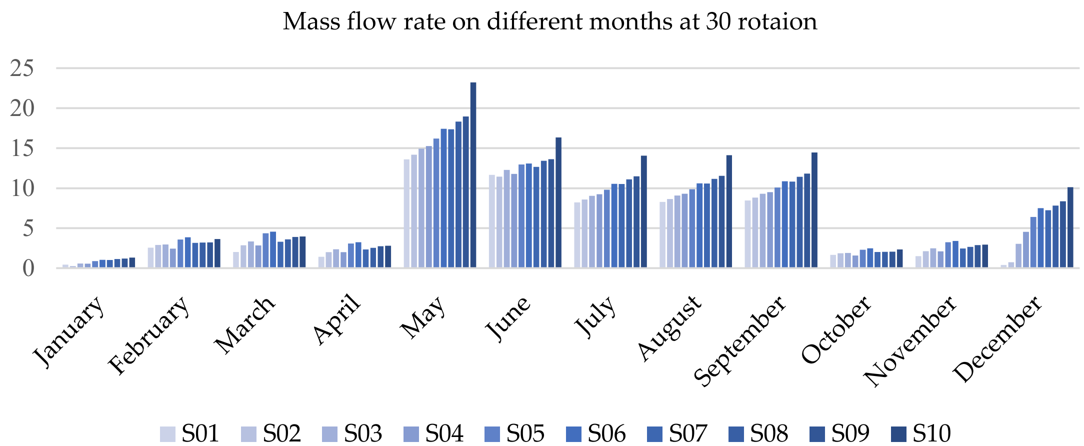

Figure 12. Mass flow rates of different segments of the tower on different months.

3.3. Scenario 03: Wind Diversion Due to Multiple Towers

In real-life scenarios, engineers might incorporate multiple towers within the structure to optimize interior space usage. In such cases, towers closer to the apertures will receive maximum wind flow, while those located in wind shadow zones will experience reduced flow. This investigation aims to demonstrate how the framework accommodates these dynamics by conducting micro-scale wind flow analysis, which can assist designers in determining more efficient tower arrangements.

For this study, four towers were placed at the center, with a center-to-center distance of 4 meters. This arrangement was purely for investigation purposes, and practical configurations may vary to accommodate technical support requirements. The team clarifies that this arrangement is hypothetical and does not reflect any company's specific design or technical advantages.

Figure 13 illustrates how the wind diverts when it encounters the first tower, reducing flow to the towers in the shadow zone. It also visualizes the decreased mass flow rate for these towers, and the accompanying chart (see Figure 14) provides a detailed analysis of the outcomes.

Preprints.org (www.preprints.org) | NOT PEER-REVIEWED | Posted: 27 March 2026 doi:10.20944/preprints202603.2179.v1

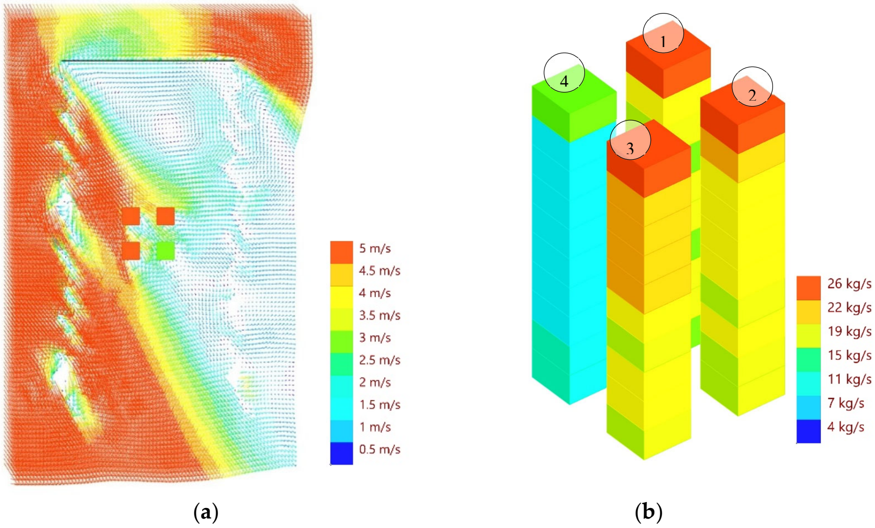

Figure 13. (**a**) Wind flow analysis for multiple towers; (**b**)Heatmap of mass flow rate for different segments of multiple towers.

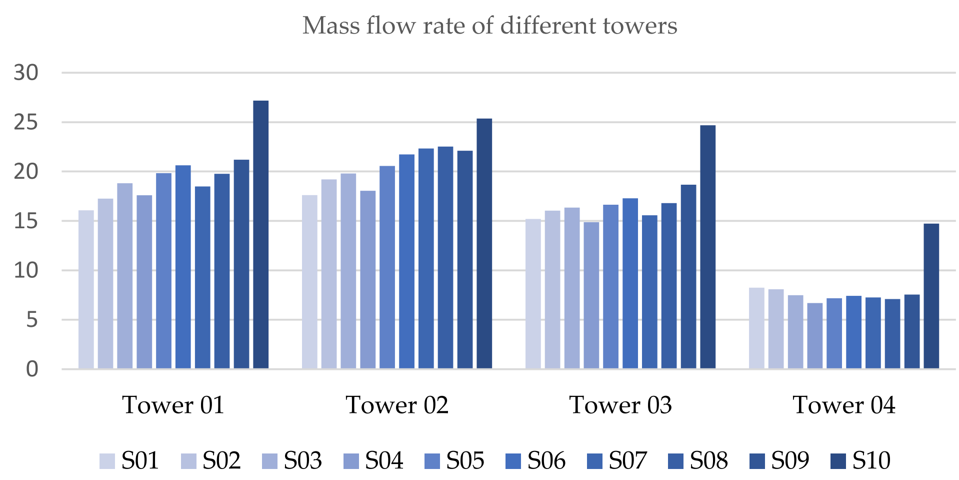

Figure 14. Mass flow rate for different segments of multiple towers.

4. Discussion

The results across all three scenarios offer deeper insights into how specific design and environmental conditions influence airflow and mass flow rate within the proposed carbon capture enclosure. Scenario 1 demonstrates that a 45-degree panel rotation yields the highest mass flow rate, indicating improved potential for carbon absorption (see Figure 9). Quantitatively, the simulations show that façade rotation can alter the total mass flow rate by up to 96.5% across the tested configurations. However, excessive airflow could introduce structural risks. The heatmap visualizations enable designers to compare options and select a rotation that achieves balanced airflow. It is important to note that this framework does not define an “ideal” airflow condition; rather, it enables performance comparisons, while the final decision must be aligned with engineering requirements and DAC system specifications.

Scenario 2 reveals that moderate and consistent mass flow is achieved between May and September (see Figure 12). Quantitatively, with a fixed façade configuration, total mass flow rates vary from approximately 8.5 kg/s in January to 169.5 kg/s in May. Interestingly, some months with high wind speed, such as February, March and December, do not correspond to higher mass flow

 doi:10.20944/preprints202603.2179.v1

rate due to the influence of design geometry. This suggests the need for adaptive design strategies to maintain airflow throughout the year.

Scenario 3 highlights the impact of spatial configuration, where Tower 4, positioned behind the others, receives the lowest mass flow due to wind shadowing. The simulations indicate that shielding effects between towers can reduce airflow by up to 60.9% compared with windward towers, demonstrating the importance of tower placement in multi-unit configurations. This also validates the workflow's ability to simulate realistic aerodynamic conditions and can inform master planning or clustering decisions in larger-scale implementations.

One limitation is that the framework does not consider the microclimate within the structure. The monthly average temperature of the site is used as a proxy, but it is important to acknowledge that the shaded structure housing the equipment may have different temperature conditions compared to the external environment. Additionally, the material properties of the equipment itself can influence interior temperatures, leading to non-uniform temperature distribution within the structure. To gain a more detailed understanding, further investigations are required to analyze the specific materials used for the carbon capture equipment.

Additionally, the simplified simulation approach does not account for pressure variations within the stack caused by air resistance, which could differ significantly from the atmospheric pressure applied at the boundary conditions. Addressing these challenges would require advanced CFD setups, which may significantly increase computational expense. The methodology adopted represents a balance between accessibility for architectural designers and the need for accurate simulations. Future updates to tools like Eddy3D that integrate these capabilities natively could improve the reliability and applicability of the proposed framework.

It is important to note that our current investigation focuses on the airflow within a single structure. However, if the technology is implemented on a larger scale, involving the master planning of multiple structures instead of just one, new challenges will arise. Nevertheless, the location of each individual structure can be optimized to ensure maximum airflow across all structures. Our team aims to implement the framework in a larger-scale context and leverage the power of design computation to explore high-performing design solutions.

While the study advances workflows for urban wind analysis, its direct contribution to carbon sequestration research is limited. The framework does not engage with the material or chemical processes of DAC technology, focusing instead on optimizing airflow for better performance. Additionally, the findings are context-specific to the chosen urban site and may not generalize to other locations without modification. Future research could integrate advanced modeling techniques to directly simulate CO2 concentrations or explore interdisciplinary collaborations to address the broader challenges of implementing DAC in urban environments.

5. Conclusions

This study presents a computational workflow that empowers architects to evaluate airflow performance in carbon capture enclosures using familiar tools such as Rhino, Grasshopper, Ladybug, and Eddy3D. By integrating mass flow rate calculations and visual analysis into early-stage design, the workflow allows designers to explore and compare multiple design options without requiring advanced CFD expertise.

Simulation results across three scenarios demonstrated the workflow's ability to respond to variations in panel orientation, seasonal wind conditions, and tower arrangements—providing performance insights that align with physical expectations. These findings support the workflow's utility in helping designers make informed decisions when integrating DAC technologies into architectural projects.

While the current framework simplifies environmental and microclimatic variables for computational efficiency, it establishes a foundation for expanding passive carbon capture strategies in architectural design. Future enhancements could include CO_2 concentration modeling, site-specific

 doi:10.20944/preprints202603.2179.v1

urban integration, and coupling with optimization algorithms to further support iterative, performance-driven design processes.

As the urgency of climate-responsive architecture grows, tools like this can help bridge the gap between environmental performance analysis and conceptual design. By streamlining airflow assessment and embedding it within common design platforms, this framework invites broader participation from the architectural community in shaping carbon-conscious solutions.

Author Contributions: Conceptualization, Md Shariful Alam and Narjes Abbasabadi; methodology, Md Shariful Alam; software, Md Shariful Alam; validation, Md Shariful Alam and Narjes Abbasabadi; formal analysis, Md Shariful Alam; investigation, Md Shariful Alam; resources, Narjes Abbasabadi; data curation, Md Shariful Alam; writing—original draft preparation, Md Shariful Alam; writing—review and editing, Narjes Abbasabadi and Md Shariful Alam; visualization, Md Shariful Alam; supervision, Narjes Abbasabadi; project administration, Narjes Abbasabadi. All authors have read and agreed to the published version of the manuscript.

Funding: This research was funded by Department of Architecture, College of Built Environment, University of Washington and Mithun.

Data Availability Statement: The data supporting the findings of this study are available from the authors upon request.

Acknowledgments: The authors would like to acknowledge the Applied Research Consortium program, organized by the College of Built Environments at the University of Washington, which supported the development of this research. The fellowship program was conducted in collaboration with the architectural design firm Mithun, whose practitioners provided valuable guidance throughout the project. The authors especially thank Jason Steiner (Mithun) for proposing the initial concept that inspired the research direction. The authors also acknowledge Katie Sage, Chi Aoyama, and Chris Reeh (Mithun) for their administrative and technical support during the development of the project. Their insights and professional feedback helped shape the practical relevance of the study. During the preparation of this manuscript, the authors used OpenAI ChatGPT (GPT-4) for assistance with language editing and improving the clarity of written text. The authors have reviewed and edited all outputs and take full responsibility for the content of this publication.

Conflicts of Interest: The authors declare no conflict of interest.

Abbreviations

The following abbreviations are used in this manuscript:

DAC	Direct Air Capture
CFD	Computational Fluid Dynamics
SSIM	Structural Similarity Index Measure
RMSE	Root Mean Square Error
ABL	Atmospheric Boundary Layer
UTCI	Universal Thermal Climate Index
CAD	Computer-Aided Design
TMYx	Typical Meteorological Year (dataset)

References

1. Keith, D.W.; Holmes, G.; St. Angelo, D.; Heidel, K. A Process for Capturing CO2 from the Atmosphere. *Joule* **2018**, *2*, 1573–1594, doi:10.1016/j.joule.2018.05.006.
2. Fasihi, M.; Efimova, O.; Breyer, C. Techno-Economic Assessment of CO2 Direct Air Capture Plants. *Journal of Cleaner Production* **2019**, *224*, 957–980, doi:10.1016/j.jclepro.2019.03.086.
3. McQueen, N.; Gomes, K.V.; McCormick, C.; Blumanthal, K.; Pisciotta, M.; Wilcox, J. A Review of Direct Air Capture (DAC): Scaling up Commercial Technologies and Innovating for the Future. *Prog. Energy* **2021**, *3*, 032001, doi:10.1088/2516-1083/abf1ce.

 doi:10.20944/preprints202603.2179.v1

4. McQueen, N.; Kelemen, P.; Dipple, G.; Renforth, P.; Wilcox, J. Ambient Weathering of Magnesium Oxide for CO2 Removal from Air. *Nat Commun* **2020**, *11*, 3299, doi:10.1038/s41467-020-16510-3.
5. Nelson, J.; McQueen, N. Heirloom: A Scalable Direct Air Capture (DAC) Process Based on Cyclic and Accelerated Weathering of Calcium Hydroxide. **2023**, *2023*, B43K-2701.
6. Heirloom A Fundamental Breakthrough in Carbon Mineralization. *Medium* 2022.
7. McQueen, N.; Samala, S.; Scholten, M. Heirloom Carbon Technologies, Inc. Final Scientific/Technical Report A Transformative Low-Cost Approach for Direct Air Mineralization of CO2 via Repeated Cycles of Ambient Weathering of Metal Oxides; Heirloom Carbon Technologies, Inc., 2022;
8. Tominaga, Y.; Mochida, A.; Yoshie, R.; Kataoka, H.; Nozu, T.; Yoshikawa, M.; Shirasawa, T. AIJ Guidelines for Practical Applications of CFD to Pedestrian Wind Environment around Buildings. *Journal of Wind Engineering and Industrial Aerodynamics* **2008**, *96*, 1749–1761, doi:10.1016/j.jweia.2008.02.058.
9. Blocken, B.; Janssen, W.D.; Van Hooff, T. CFD Simulation for Pedestrian Wind Comfort and Wind Safety in Urban Areas: General Decision Framework and Case Study for the Eindhoven University Campus. *Environmental Modelling & Software* **2012**, *30*, 15–34, doi:10.1016/j.envsoft.2011.11.009.
10. Rahimi, S.; Alvarez, M.; Berardi, U.; Stone, B.; Kastner, P. Coupled Urban Physics in Microclimate Modeling: Validating and Enhancing Simulation Tools. *Building and Environment* **2025**, *285*, 113637, doi:10.1016/j.buildenv.2025.113637.
11. Mirzabeigi, S.; Razkenari, M. Design Optimization of Urban Typologies: A Framework for Evaluating Building Energy Performance and Outdoor Thermal Comfort. *Sustainable Cities and Society* **2022**, *76*, 103515, doi:10.1016/j.scs.2021.103515.
12. Toparlar, Y.; Blocken, B.; Maiheu, B.; van Heijst, G.J.F. A Review on the CFD Analysis of Urban Microclimate. *Renewable and Sustainable Energy Reviews* **2017**, *80*, 1613–1640, doi:10.1016/j.rser.2017.05.248.
13. Albatayneh, A.; Alterman, D.; Page, A. Adaptation the Use of CFD Modelling for Building Thermal Simulation.; January 4 2018; pp. 68–72.
14. Hu, Y.; Peng, Y.; Gao, Z.; Xu, F. Application of CFD Plug-Ins Integrated into Urban and Building Design Platforms for Performance Simulations: A Literature Review. *Frontiers of Architectural Research* **2023**, *12*, 148–174, doi:10.1016/j.foar.2022.06.005.
15. Kaijima, S.; Bouffanais, R.; Willcox, K.; Naidu, S. Computational Fluid Dynamics for Architectural Design. *Architectural Design* **2013**, *83*, doi:10.1002/ad.1566.
16. Weller, H.G.; Tabor, G.; Jasak, H.; Fureby, C. A Tensorial Approach to Computational Continuum Mechanics Using Object-Oriented Techniques. *Computer in Physics* **1998**, *12*, 620–631, doi:10.1063/1.168744.
17. Jasak, H.; Jemcov, A.; Tukovic, Z. OpenFOAM: A C++ Library for Complex Physics Simulations. **2013**.
18. Kastner, P.; Dogan, T. Eddy3D: A Toolkit for Decoupled Outdoor Thermal Comfort Simulations in Urban Areas. *Building and Environment* **2021**, *212*, 108639, doi:10.1016/j.buildenv.2021.108639.
19. Dogan, T.; Kastner, P. Streamlined CFD Simulation Framework to Generate Wind-Pressure Coefficients on Building Facades for Airflow Network Simulations. *Build. Simul.* **2021**, *14*, 1189–1200, doi:10.1007/s12273-020-0727-x.
20. Young, E.; Kastner, P.; Dogan, T.; Chokhachian, A.; Mokhtar, S.; Reinhart, C. Modeling Outdoor Thermal Comfort along Cycling Routes at Varying Levels of Physical Accuracy to Predict Bike Ridership in Cambridge, MA. *Building and Environment* **2021**, *208*, 108577, doi:10.1016/j.buildenv.2021.108577.
21. Kastner, P.; Dogan, T. A GAN-Based Surrogate Model for Instantaneous Urban Wind Flow Prediction. *Building and Environment* **2023**, *242*, 110384, doi:10.1016/j.buildenv.2023.110384.
22. Li, Y.; Yi, Y.K. Optimal Shape Design Using Machine Learning for Wind Energy and Pressure. *Journal of Building Engineering* **2023**, *70*, 106337, doi:10.1016/j.jobe.2023.106337.

doi:10.20944/preprints202603.2179.v1

23. Estrado, E.; Turrin, M.; Eigenraam, P. Optimization of Complex-Geometry High-Rise Buildings Based on Wind Load Analysis. *SIMULATION* **2022**, 003754972211095, doi:10.1177/00375497221109577.
24. Autodesk Flow Design - How to Set Up Models; 2014;